BABAR-PUB-07/072
SLAC-PUB-13229

Measurement of the CKM angle γ in $B^0 \to \overline{D}^0(D^0)K^{*0}$ with a Dalitz analysis of $D^0 \to K_S\pi^+\pi^-$

B. Aubert,[1] M. Bona,[1] Y. Karyotakis,[1] J. P. Lees,[1] V. Poireau,[1] X. Prudent,[1] V. Tisserand,[1] A. Zghiche,[1] J. Garra Tico,[2] E. Grauges,[2] L. Lopez,[3] A. Palano,[3] M. Pappagallo,[3] G. Eigen,[4] B. Stugu,[4] L. Sun,[4] G. S. Abrams,[5] M. Battaglia,[5] D. N. Brown,[5] J. Button-Shafer,[5] R. N. Cahn,[5] R. G. Jacobsen,[5] J. A. Kadyk,[5] L. T. Kerth,[5] Yu. G. Kolomensky,[5] G. Kukartsev,[5] G. Lynch,[5] I. L. Osipenkov,[5] M. T. Ronan,[5, *] K. Tackmann,[5] T. Tanabe,[5] W. A. Wenzel,[5] C. M. Hawkes,[6] N. Soni,[6] A. T. Watson,[6] H. Koch,[7] T. Schroeder,[7] D. Walker,[8] D. J. Asgeirsson,[9] T. Cuhadar-Donszelmann,[9] B. G. Fulsom,[9] C. Hearty,[9] T. S. Mattison,[9] J. A. McKenna,[9] M. Barrett,[10] A. Khan,[10] M. Saleem,[10] L. Teodorescu,[10] V. E. Blinov,[11] A. D. Bukin,[11] A. R. Buzykaev,[11] V. P. Druzhinin,[11] V. B. Golubev,[11] A. P. Onuchin,[11] S. I. Serednyakov,[11] Yu. I. Skovpen,[11] E. P. Solodov,[11] K. Yu. Todyshev,[11] M. Bondioli,[12] S. Curry,[12] I. Eschrich,[12] D. Kirkby,[12] A. J. Lankford,[12] P. Lund,[12] M. Mandelkern,[12] E. C. Martin,[12] D. P. Stoker,[12] S. Abachi,[13] C. Buchanan,[13] J. W. Gary,[14] F. Liu,[14] O. Long,[14] B. C. Shen,[14, *] G. M. Vitug,[14] Z. Yasin,[14] L. Zhang,[14] H. P. Paar,[15] S. Rahatlou,[15] V. Sharma,[15] C. Campagnari,[16] T. M. Hong,[16] D. Kovalskyi,[16] M. A. Mazur,[16] J. D. Richman,[16] T. W. Beck,[17] A. M. Eisner,[17] C. J. Flacco,[17] C. A. Heusch,[17] J. Kroseberg,[17] W. S. Lockman,[17] T. Schalk,[17] B. A. Schumm,[17] A. Seiden,[17] M. G. Wilson,[17] L. O. Winstrom,[17] E. Chen,[18] C. H. Cheng,[18] D. A. Doll,[18] B. Echenard,[18] F. Fang,[18] D. G. Hitlin,[18] I. Narsky,[18] T. Piatenko,[18] F. C. Porter,[18] R. Andreassen,[19] G. Mancinelli,[19] B. T. Meadows,[19] K. Mishra,[19] M. D. Sokoloff,[19] F. Blanc,[20] P. C. Bloom,[20] W. T. Ford,[20] J. F. Hirschauer,[20] A. Kreisel,[20] M. Nagel,[20] U. Nauenberg,[20] A. Olivas,[20] J. G. Smith,[20] K. A. Ulmer,[20] S. R. Wagner,[20] R. Ayad,[21, †] A. M. Gabareen,[21] A. Soffer,[21, ‡] W. H. Toki,[21] R. J. Wilson,[21] D. D. Altenburg,[22] E. Feltresi,[22] A. Hauke,[22] H. Jasper,[22] M. Karbach,[22] J. Merkel,[22] A. Petzold,[22] B. Spaan,[22] K. Wacker,[22] V. Klose,[23] M. J. Kobel,[23] H. M. Lacker,[23] W. F. Mader,[23] R. Nogowski,[23] J. Schubert,[23] K. R. Schubert,[23] R. Schwierz,[23] J. E. Sundermann,[23] A. Volk,[23] D. Bernard,[24] G. R. Bonneaud,[24] E. Latour,[24] Ch. Thiebaux,[24] M. Verderi,[24] P. J. Clark,[25] W. Gradl,[25] S. Playfer,[25] A. I. Robertson,[25] J. E. Watson,[25] M. Andreotti,[26] D. Bettoni,[26] C. Bozzi,[26] R. Calabrese,[26] A. Cecchi,[26] G. Cibinetto,[26] P. Franchini,[26] E. Luppi,[26] M. Negrini,[26] A. Petrella,[26] L. Piemontese,[26] E. Prencipe,[26] V. Santoro,[26] F. Anulli,[27] R. Baldini-Ferroli,[27] A. Calcaterra,[27] R. de Sangro,[27] G. Finocchiaro,[27] S. Pacetti,[27] P. Patteri,[27] I. M. Peruzzi,[27, §] M. Piccolo,[27] M. Rama,[27] A. Zallo,[27] A. Buzzo,[28] R. Contri,[28] M. Lo Vetere,[28] M. M. Macri,[28] M. R. Monge,[28] S. Passaggio,[28] C. Patrignani,[28] E. Robutti,[28] A. Santroni,[28] S. Tosi,[28] K. S. Chaisanguanthum,[29] M. Morii,[29] R. S. Dubitzky,[30] J. Marks,[30] S. Schenk,[30] U. Uwer,[30] D. J. Bard,[31] P. D. Dauncey,[31] J. A. Nash,[31] W. Panduro Vazquez,[31] M. Tibbetts,[31] P. K. Behera,[32] X. Chai,[32] M. J. Charles,[32] U. Mallik,[32] J. Cochran,[33] H. B. Crawley,[33] L. Dong,[33] V. Eyges,[33] W. T. Meyer,[33] S. Prell,[33] E. I. Rosenberg,[33] A. E. Rubin,[33] Y. Y. Gao,[34] A. V. Gritsan,[34] Z. J. Guo,[34] C. K. Lae,[34] A. G. Denig,[35] M. Fritsch,[35] G. Schott,[35] N. Arnaud,[36] J. Béquilleux,[36] A. D'Orazio,[36] M. Davier,[36] J. Firmino da Costa,[36] G. Grosdidier,[36] A. Höcker,[36] V. Lepeltier,[36] F. Le Diberder,[36] A. M. Lutz,[36] S. Pruvot,[36] P. Roudeau,[36] M. H. Schune,[36] J. Serrano,[36] V. Sordini,[36] A. Stocchi,[36] W. F. Wang,[36] G. Wormser,[36] D. J. Lange,[37] D. M. Wright,[37] I. Bingham,[38] J. P. Burke,[38] C. A. Chavez,[38] J. R. Fry,[38] E. Gabathuler,[38] R. Gamet,[38] D. E. Hutchcroft,[38] D. J. Payne,[38] C. Touramanis,[38] A. J. Bevan,[39] K. A. George,[39] F. Di Lodovico,[39] R. Sacco,[39] M. Sigamani,[39] G. Cowan,[40] H. U. Flaecher,[40] D. A. Hopkins,[40] S. Paramesvaran,[40] F. Salvatore,[40] A. C. Wren,[40] D. N. Brown,[41] C. L. Davis,[41] K. E. Alwyn,[42] N. R. Barlow,[42] R. J. Barlow,[42] Y. M. Chia,[42] C. L. Edgar,[42] G. D. Lafferty,[42] T. J. West,[42] J. I. Yi,[42] J. Anderson,[43] C. Chen,[43] A. Jawahery,[43] D. A. Roberts,[43] G. Simi,[43] J. M. Tuggle,[43] C. Dallapiccola,[44] S. S. Hertzbach,[44] X. Li,[44] E. Salvati,[44] S. Saremi,[44] R. Cowan,[45] D. Dujmic,[45] P. H. Fisher,[45] K. Koeneke,[45] G. Sciolla,[45] M. Spitznagel,[45] F. Taylor,[45] R. K. Yamamoto,[45] M. Zhao,[45] S. E. Mclachlin,[46, *] P. M. Patel,[46] S. H. Robertson,[46] A. Lazzaro,[47] V. Lombardo,[47] F. Palombo,[47] J. M. Bauer,[48] L. Cremaldi,[48] V. Eschenburg,[48] R. Godang,[48] R. Kroeger,[48] D. A. Sanders,[48] D. J. Summers,[48] H. W. Zhao,[48] S. Brunet,[49] D. Côté,[49] M. Simard,[49] P. Taras,[49] F. B. Viaud,[49] H. Nicholson,[50] G. De Nardo,[51] L. Lista,[51] D. Monorchio,[51] C. Sciacca,[51] M. A. Baak,[52] G. Raven,[52] H. L. Snoek,[52] C. P. Jessop,[53] K. J. Knoepfel,[53] J. M. LoSecco,[53] G. Benelli,[54] L. A. Corwin,[54] K. Honscheid,[54] H. Kagan,[54] R. Kass,[54] J. P. Morris,[54] A. M. Rahimi,[54] J. J. Regensburger,[54] S. J. Sekula,[54] Q. K. Wong,[54] N. L. Blount,[55] J. Brau,[55]

Submitted to Physical Review D

Work supported in part by US Department of Energy contract DE-AC02-76SF00515

R. Frey,[55] O. Igonkina,[55] J. A. Kolb,[55] M. Lu,[55] R. Rahmat,[55] N. B. Sinev,[55] D. Strom,[55] J. Strube,[55]
E. Torrence,[55] G. Castelli,[56] N. Gagliardi,[56] A. Gaz,[56] M. Margoni,[56] M. Morandin,[56] M. Posocco,[56] M. Rotondo,[56]
F. Simonetto,[56] R. Stroili,[56] C. Voci,[56] P. del Amo Sanchez,[57] E. Ben-Haim,[57] H. Briand,[57] G. Calderini,[57]
J. Chauveau,[57] P. David,[57] L. Del Buono,[57] O. Hamon,[57] Ph. Leruste,[57] J. Malclès,[57] J. Ocariz,[57] A. Perez,[57]
J. Prendki,[57] L. Gladney,[58] M. Biasini,[59] R. Covarelli,[59] E. Manoni,[59] C. Angelini,[60] G. Batignani,[60] S. Bettarini,[60]
M. Carpinelli,[60, ¶] A. Cervelli,[60] F. Forti,[60] M. A. Giorgi,[60] A. Lusiani,[60] G. Marchiori,[60] M. Morganti,[60]
N. Neri,[60] E. Paoloni,[60] G. Rizzo,[60] J. J. Walsh,[60] J. Biesiada,[61] Y. P. Lau,[61] D. Lopes Pegna,[61] C. Lu,[61]
J. Olsen,[61] A. J. S. Smith,[61] A. V. Telnov,[61] E. Baracchini,[62] G. Cavoto,[62] D. del Re,[62] E. Di Marco,[62]
R. Faccini,[62] F. Ferrarotto,[62] F. Ferroni,[62] M. Gaspero,[62] P. D. Jackson,[62] M. A. Mazzoni,[62] S. Morganti,[62]
G. Piredda,[62] F. Polci,[62] F. Renga,[62] C. Voena,[62] M. Ebert,[63] T. Hartmann,[63] H. Schröder,[63] R. Waldi,[63]
T. Adye,[64] B. Franek,[64] E. O. Olaiya,[64] W. Roethel,[64] F. F. Wilson,[64] S. Emery,[65] M. Escalier,[65]
A. Gaidot,[65] S. F. Ganzhur,[65] G. Hamel de Monchenault,[65] W. Kozanecki,[65] G. Vasseur,[65] Ch. Yèche,[65]
M. Zito,[65] X. R. Chen,[66] H. Liu,[66] W. Park,[66] M. V. Purohit,[66] R. M. White,[66] J. R. Wilson,[66] M. T. Allen,[67]
D. Aston,[67] R. Bartoldus,[67] P. Bechtle,[67] J. F. Benitez,[67] R. Cenci,[67] J. P. Coleman,[67] M. R. Convery,[67]
J. C. Dingfelder,[67] J. Dorfan,[67] G. P. Dubois-Felsmann,[67] W. Dunwoodie,[67] R. C. Field,[67] T. Glanzman,[67]
S. J. Gowdy,[67] M. T. Graham,[67] P. Grenier,[67] C. Hast,[67] W. R. Innes,[67] J. Kaminski,[67] M. H. Kelsey,[67] H. Kim,[67]
P. Kim,[67] M. L. Kocian,[67] D. W. G. S. Leith,[67] S. Li,[67] B. Lindquist,[67] S. Luitz,[67] V. Luth,[67] H. L. Lynch,[67]
D. B. MacFarlane,[67] H. Marsiske,[67] R. Messner,[67] D. R. Muller,[67] H. Neal,[67] S. Nelson,[67] C. P. O'Grady,[67]
I. Ofte,[67] A. Perazzo,[67] M. Perl,[67] B. N. Ratcliff,[67] A. Roodman,[67] A. A. Salnikov,[67] R. H. Schindler,[67]
J. Schwiening,[67] A. Snyder,[67] D. Su,[67] M. K. Sullivan,[67] K. Suzuki,[67] S. K. Swain,[67] J. M. Thompson,[67]
J. Va'vra,[67] A. P. Wagner,[67] M. Weaver,[67] W. J. Wisniewski,[67] M. Wittgen,[67] D. H. Wright,[67] H. W. Wulsin,[67]
A. K. Yarritu,[67] K. Yi,[67] C. C. Young,[67] V. Ziegler,[67] P. R. Burchat,[68] A. J. Edwards,[68] S. A. Majewski,[68]
T. S. Miyashita,[68] B. A. Petersen,[68] L. Wilden,[68] S. Ahmed,[69] M. S. Alam,[69] R. Bula,[69] J. A. Ernst,[69] B. Pan,[69]
M. A. Saeed,[69] S. B. Zain,[69] S. M. Spanier,[70] B. J. Wogsland,[70] R. Eckmann,[71] J. L. Ritchie,[71] A. M. Ruland,[71]
C. J. Schilling,[71] R. F. Schwitters,[71] J. M. Izen,[72] X. C. Lou,[72] S. Ye,[72] F. Bianchi,[73] D. Gamba,[73]
M. Pelliccioni,[73] M. Bomben,[74] L. Bosisio,[74] C. Cartaro,[74] F. Cossutti,[74] G. Della Ricca,[74] L. Lanceri,[74]
L. Vitale,[74] V. Azzolini,[75] N. Lopez-March,[75] F. Martinez-Vidal,[75] D. A. Milanes,[75] A. Oyanguren,[75] J. Albert,[76]
Sw. Banerjee,[76] B. Bhuyan,[76] K. Hamano,[76] R. Kowalewski,[76] I. M. Nugent,[76] J. M. Roney,[76] R. J. Sobie,[76]
T. J. Gershon,[77] P. F. Harrison,[77] J. Ilic,[77] T. E. Latham,[77] G. B. Mohanty,[77] H. R. Band,[78] X. Chen,[78]
S. Dasu,[78] K. T. Flood,[78] P. E. Kutter,[78] Y. Pan,[78] M. Pierini,[78] R. Prepost,[78] C. O. Vuosalo,[78] and S. L. Wu[78]
(The *BABAR* Collaboration)

[1]Laboratoire de Physique des Particules, IN2P3/CNRS et Université de Savoie, F-74941 Annecy-Le-Vieux, France
[2]Universitat de Barcelona, Facultat de Fisica, Departament ECM, E-08028 Barcelona, Spain
[3]Università di Bari, Dipartimento di Fisica and INFN, I-70126 Bari, Italy
[4]University of Bergen, Institute of Physics, N-5007 Bergen, Norway
[5]Lawrence Berkeley National Laboratory and University of California, Berkeley, California 94720, USA
[6]University of Birmingham, Birmingham, B15 2TT, United Kingdom
[7]Ruhr Universität Bochum, Institut für Experimentalphysik 1, D-44780 Bochum, Germany
[8]University of Bristol, Bristol BS8 1TL, United Kingdom
[9]University of British Columbia, Vancouver, British Columbia, Canada V6T 1Z1
[10]Brunel University, Uxbridge, Middlesex UB8 3PH, United Kingdom
[11]Budker Institute of Nuclear Physics, Novosibirsk 630090, Russia
[12]University of California at Irvine, Irvine, California 92697, USA
[13]University of California at Los Angeles, Los Angeles, California 90024, USA
[14]University of California at Riverside, Riverside, California 92521, USA
[15]University of California at San Diego, La Jolla, California 92093, USA
[16]University of California at Santa Barbara, Santa Barbara, California 93106, USA
[17]University of California at Santa Cruz, Institute for Particle Physics, Santa Cruz, California 95064, USA
[18]California Institute of Technology, Pasadena, California 91125, USA
[19]University of Cincinnati, Cincinnati, Ohio 45221, USA
[20]University of Colorado, Boulder, Colorado 80309, USA
[21]Colorado State University, Fort Collins, Colorado 80523, USA
[22]Universität Dortmund, Institut für Physik, D-44221 Dortmund, Germany
[23]Technische Universität Dresden, Institut für Kern- und Teilchenphysik, D-01062 Dresden, Germany
[24]Laboratoire Leprince-Ringuet, CNRS/IN2P3, Ecole Polytechnique, F-91128 Palaiseau, France
[25]University of Edinburgh, Edinburgh EH9 3JZ, United Kingdom

[26]Università di Ferrara, Dipartimento di Fisica and INFN, I-44100 Ferrara, Italy
[27]Laboratori Nazionali di Frascati dell'INFN, I-00044 Frascati, Italy
[28]Università di Genova, Dipartimento di Fisica and INFN, I-16146 Genova, Italy
[29]Harvard University, Cambridge, Massachusetts 02138, USA
[30]Universität Heidelberg, Physikalisches Institut, Philosophenweg 12, D-69120 Heidelberg, Germany
[31]Imperial College London, London, SW7 2AZ, United Kingdom
[32]University of Iowa, Iowa City, Iowa 52242, USA
[33]Iowa State University, Ames, Iowa 50011-3160, USA
[34]Johns Hopkins University, Baltimore, Maryland 21218, USA
[35]Universität Karlsruhe, Institut für Experimentelle Kernphysik, D-76021 Karlsruhe, Germany
[36]Laboratoire de l'Accélérateur Linéaire, IN2P3/CNRS et Université Paris-Sud 11,
Centre Scientifique d'Orsay, B. P. 34, F-91898 ORSAY Cedex, France
[37]Lawrence Livermore National Laboratory, Livermore, California 94550, USA
[38]University of Liverpool, Liverpool L69 7ZE, United Kingdom
[39]Queen Mary, University of London, E1 4NS, United Kingdom
[40]University of London, Royal Holloway and Bedford New College, Egham, Surrey TW20 0EX, United Kingdom
[41]University of Louisville, Louisville, Kentucky 40292, USA
[42]University of Manchester, Manchester M13 9PL, United Kingdom
[43]University of Maryland, College Park, Maryland 20742, USA
[44]University of Massachusetts, Amherst, Massachusetts 01003, USA
[45]Massachusetts Institute of Technology, Laboratory for Nuclear Science, Cambridge, Massachusetts 02139, USA
[46]McGill University, Montréal, Québec, Canada H3A 2T8
[47]Università di Milano, Dipartimento di Fisica and INFN, I-20133 Milano, Italy
[48]University of Mississippi, University, Mississippi 38677, USA
[49]Université de Montréal, Physique des Particules, Montréal, Québec, Canada H3C 3J7
[50]Mount Holyoke College, South Hadley, Massachusetts 01075, USA
[51]Università di Napoli Federico II, Dipartimento di Scienze Fisiche and INFN, I-80126, Napoli, Italy
[52]NIKHEF, National Institute for Nuclear Physics and High Energy Physics, NL-1009 DB Amsterdam, The Netherlands
[53]University of Notre Dame, Notre Dame, Indiana 46556, USA
[54]Ohio State University, Columbus, Ohio 43210, USA
[55]University of Oregon, Eugene, Oregon 97403, USA
[56]Università di Padova, Dipartimento di Fisica and INFN, I-35131 Padova, Italy
[57]Laboratoire de Physique Nucléaire et de Hautes Energies,
IN2P3/CNRS, Université Pierre et Marie Curie-Paris6,
Université Denis Diderot-Paris7, F-75252 Paris, France
[58]University of Pennsylvania, Philadelphia, Pennsylvania 19104, USA
[59]Università di Perugia, Dipartimento di Fisica and INFN, I-06100 Perugia, Italy
[60]Università di Pisa, Dipartimento di Fisica, Scuola Normale Superiore and INFN, I-56127 Pisa, Italy
[61]Princeton University, Princeton, New Jersey 08544, USA
[62]Università di Roma La Sapienza, Dipartimento di Fisica and INFN, I-00185 Roma, Italy
[63]Universität Rostock, D-18051 Rostock, Germany
[64]Rutherford Appleton Laboratory, Chilton, Didcot, Oxon, OX11 0QX, United Kingdom
[65]DSM/Dapnia, CEA/Saclay, F-91191 Gif-sur-Yvette, France
[66]University of South Carolina, Columbia, South Carolina 29208, USA
[67]Stanford Linear Accelerator Center, Stanford, California 94309, USA
[68]Stanford University, Stanford, California 94305-4060, USA
[69]State University of New York, Albany, New York 12222, USA
[70]University of Tennessee, Knoxville, Tennessee 37996, USA
[71]University of Texas at Austin, Austin, Texas 78712, USA
[72]University of Texas at Dallas, Richardson, Texas 75083, USA
[73]Università di Torino, Dipartimento di Fisica Sperimentale and INFN, I-10125 Torino, Italy
[74]Università di Trieste, Dipartimento di Fisica and INFN, I-34127 Trieste, Italy
[75]IFIC, Universitat de Valencia-CSIC, E-46071 Valencia, Spain
[76]University of Victoria, Victoria, British Columbia, Canada V8W 3P6
[77]Department of Physics, University of Warwick, Coventry CV4 7AL, United Kingdom
[78]University of Wisconsin, Madison, Wisconsin 53706, USA

(Dated: May 14, 2008)

We present a measurement of the angle γ of the Unitarity Triangle with a Dalitz analysis of neutral D decays to $K_S\pi^+\pi^-$ from the processes $B^0 \to \overline{D}^0(D^0)K^{*0}$ ($\overline{B}^0 \to D^0(\overline{D}^0)\overline{K}^{*0}$) with $K^{*0} \to K^+\pi^-$ ($\overline{K}^{*0} \to K^-\pi^+$). Using a sample of 371×10^6 $B\bar{B}$ pairs collected with the *BABAR* detector at PEP II, we measure the angle γ as a function of r_S, the magnitude of the average ratio between $b \to u$ and $b \to c$ amplitudes. Combining this result with the available information on r_S, we obtain $\gamma = (162 \pm 56)^\circ$ or $(342 \pm 56)^\circ$ and $r_S < 0.55$ at 95% probability.

PACS numbers: 13.25.Hw, 14.40.Nd

Various methods have been proposed to determine the Unitarity Triangle angle γ [1, 2] of the Cabibbo-Kobayashi-Maskawa (CKM) quark mixing matrix [3] using $B^- \to \tilde{D}^{0(*)}K^{(*)-}$ decays, where the symbol $\tilde{D}^{0(*)}$ indicates either a $D^{0(*)}$ or a $\overline{D}^{0(*)}$ meson. A B^- can decay into a $\tilde{D}^{0(*)}K^{(*)-}$ final state via a $b \to c$ or a $b \to u$ mediated process and *CP* violation can be detected when the $D^{0(*)}$ and the $\overline{D}^{0(*)}$ decay to the same final state. These processes are thus sensitive to $\gamma = \arg\{-V^*_{ub}V_{ud}/V^*_{cb}V_{cd}\}$

In this paper we present the first measurement of the angle γ using neutral B meson decays. We reconstruct $B^0 \to \tilde{D}^0K^{*0}$, with $K^{*0} \to K^+\pi^-$ (charge conjugate processes are assumed throughout the paper and K^{*0} refers to $K^*(892)^0$), where the flavor of the B meson is identified by the kaon electric charge. Neutral D mesons are reconstructed in the $K_S\pi^+\pi^-$ decay mode and are analyzed with the Dalitz technique [2]. The final states we reconstruct can be reached through $b \to c$ and $b \to u$ processes with the diagrams shown in Fig. 1.

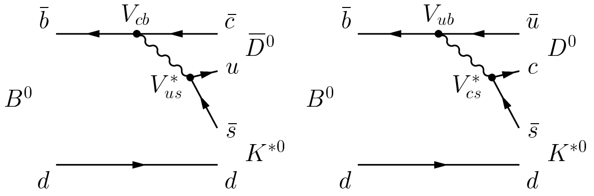

FIG. 1: Feynman diagrams for $B^0 \to \overline{D}^0K^{*0}$ (left, $\bar{b} \to \bar{c}$ transition) and $B^0 \to D^0K^{*0}$ (right, $\bar{b} \to \bar{u}$ transition). A K^{*0} is a decay product of a B^0 while a $\overline{K}^{*0}$ results from a $\overline{B}^0$ decay. Note that $b \to u$ or $\bar{b} \to \bar{u}$ transitions always lead to a $D^0K^+\pi^-$ or to a $\overline{D}^0K^-\pi^+$ final state.

When analyzing $B^0 \to \tilde{D}^0K^{*0}$ decays, the natural width of the K^{*0} (50 MeV/c^2) has to be considered. In the K^{*0} mass region, amplitudes for decays to higher-mass $K\pi$ resonances interfere with the signal decay amplitude and with each other. For this analysis we use effective variables, introduced in Ref. [4], obtained by integrating over a region of the $B^0 \to \tilde{D}^0K^+\pi^-$ Dalitz plot corresponding to the K^{*0} . For this purpose we introduce the quantities r_S, k, and δ_S defined as

$$r_S^2 \equiv \frac{\Gamma(B^0 \to D^0K^+\pi^-)}{\Gamma(B^0 \to \overline{D}^0K^+\pi^-)} = \frac{\int dp\ A_u^2(p)}{\int dp\ A_c^2(p)}, \qquad (1)$$

$$ke^{i\delta_S} \equiv \frac{\int dp\ A_c(p)A_u(p)e^{i\delta(p)}}{\sqrt{\int dp\ A_c^2(p)\ \int dp\ A_u^2(p)}}, \qquad (2)$$

where $0 \leq k \leq 1$ and $\delta_S \in [0, 2\pi]$. The amplitudes for the $b \to c$ and $b \to u$ transitions, $A_c(p)$ and $A_u(p)$, are real and positive and $\delta(p)$ is the relative strong phase. The variable p indicates the position in the $\tilde{D}^0K^+\pi^-$ Dalitz plot. In case of a two-body B decay, r_S and δ_S become $r_B = |A_u|/|A_c|$ and δ_B (the strong phase difference between A_u and A_c) and $k = 1$. Because of CKM factors and the fact that both diagrams, for the neutral B decays we consider, are color-suppressed, the average amplitude ratio r_S in $B^0 \to \tilde{D}^0K^{*0}$ is expected to be in the range [0.3, 0.5], larger than the analogous ratio for the charged B (which is of the order of 10% [5]). An earlier measurement sets an upper limit $r_S < 0.4$ at 90% probability [6]. A phenomenological approach [7] proposed to evaluate r_B in the $B^0 \to \tilde{D}^0K^0$ system gives $r_B = 0.27 \pm 0.18$.

The analysis presented in this paper uses a data sample of 371×10^6 $B\bar{B}$ pairs collected with the *BABAR* detector at the PEP-II storage ring. The *BABAR* detector is described elsewhere [8].

We reconstruct $B^0 \to \tilde{D}^0K^{*0}$ events with $K^{*0} \to K^+\pi^-$ and $\tilde{D}^0 \to K_S\pi^+\pi^-$. The K_S is reconstructed from pairs of oppositely-charged pions with invariant mass within 7 MeV/c^2 of the nominal K_S mass [9]. We also require that $\cos\alpha_{K_S}(\tilde{D}^0) > 0.997$, where $\alpha_{K_S}(\tilde{D}^0)$ is the angle between the K_S line of flight (line between the $\tilde{D}^0$ and the K_S decay points) and the K_S momentum (measured from the two pion momenta). Neutral D candidates are selected by combining K_S candidates with two oppositely-charged pion candidates and requiring the $\tilde{D}^0$ invariant mass to be within 11 MeV/c^2 of its nominal mass [9]. The K_S and the two pions used to reconstruct the $\tilde{D}^0$ are constrained to originate from a common vertex. Charged kaon identification, based on Cherenkov angle and dE/dx measurements, is required for the charged K. The tracks used to reconstruct the K^{*0} are constrained to originate from a common vertex and their invariant mass is required to lie within 48 MeV/c^2 of the nominal K^{*0} mass [9]. We define θ_{Hel} as the angle between the direction of flight of the charged K in the K^{*0} rest frame with respect to the direction of flight of the K^{*0} in the B rest frame. We require $|\cos\theta_{Hel}| > 0.3$. The B^0 candidates are reconstructed by combining one $\tilde{D}^0$ and one K^{*0} candidate, constraining them to originate from a common vertex. We also require the absolute value of the cosine of the B polar angle with respect to the beam axis in the e^+e^- center of mass (CM) frame to be less than 0.9.

We measure two almost independent kinematic variables: the beam-energy substituted mass $m_{\rm ES} \equiv \sqrt{(E_0^{*2}/2 + \vec{p_0} \cdot \vec{p_B})^2/E_0^2 - {p_B}^2}$, and the energy difference $\Delta E \equiv E_B^* - E_0^*/2$, where E and p are energy and momentum, the subscripts B and 0 refer to the candidate B and to the e^+e^- system respectively and the asterisk denotes the e^+e^- CM frame. The B candidates are required to have ΔE in the range $[-0.025, 0.025]$ GeV, and $m_{\rm ES}$ in the range $[5.2, 5.29]$ GeV/c^2 .

In less than 1% of the cases, multiple candidates are present in the same event and we choose the one with reconstructed $\tilde{D}^0$ mass closest to the nominal mass [9]. In the case of two B candidates reconstructed from the same $\tilde{D}^0$, we choose the candidate with the largest absolute value of $\cos\theta_{Hel}$. The overall reconstruction and selection efficiency for signal events in Monte Carlo simulation (MC) is $(10.8 \pm 0.5)\%$.

After applying the selection criteria described above, the background is composed of continuum events ($e^+e^- \rightarrow q\bar{q}$, $q = u, d, s, c$) and $\Upsilon(4\mathrm{S}) \rightarrow B\bar{B}$ events ("$B\bar{B}$", in the following). To discriminate against the continuum background events (the dominant background component), which, in contrast to $B\bar{B}$ events, have a jet-like shape, we use a Fisher discriminant $\mathcal{F}$ [10]. The discriminant $\mathcal{F}$ is a linear combination of three variables: $\cos\theta_{thrust}$, the cosine of the angle between the B thrust axis and the thrust axis of the rest of the event, $L_0 = \sum_i p_i$, and $L_2 = \sum_i p_i |\cos\theta_i|^2$. Here, p_i is the momentum and θ_i is the angle with respect to the thrust axis of the B candidate. The index i runs over all the reconstructed tracks and energy deposits in the calorimeter not associated with a track. The tracks and energy deposits used to reconstruct the B are excluded from these sums. All these variables are calculated in the e^+e^- CM frame. The coefficients of the Fisher discriminant, chosen to maximize the separation between signal and continuum background, are determined using a sample of simulated signal events and 35 fb^{-1} of continuum events from data collected at an e^+e^- CM energy 40 MeV below the $\Upsilon(4S)$ resonance (off-resonance).

To further discriminate the signal from the continuum events we use the proper time interval Δt between the two B decays. This is calculated from the measured separation, Δz, between the decay points of the reconstructed B ($B_{\rm rec}$) and the other B ($B_{\rm oth}$) along the beam direction. The $B_{\rm rec}$ decay point is the common vertex of the B decay products. The $B_{\rm oth}$ decay point is obtained using tracks which do not belong to $B_{\rm rec}$ and imposing constraints from the $B_{\rm rec}$ momentum and the beam-spot location.

Background events for which the reconstructed K_S, π^+, and π^- come from a real $\tilde{D}^0$ ("true D^0", in the following) are treated separately because of their distribution over the $\tilde{D}^0$ Dalitz plane. A fit to the $K_S\pi^+\pi^-$ invariant mass distribution for events in the $m_{\rm ES}$ sideband ($m_{\rm ES} < 5.27\,\mathrm{GeV}/c^2$) has been performed on data to obtain the fraction of true D^0 equal to 0.289 ± 0.028. This value is in agreement with that determined from simulated $B\bar{B}$ and continuum background samples. Background events with final states containing $D^0h^+\pi^-$ or $\overline{D}^0h^-\pi^+$, where $h^\pm$ is a candidate $K^\pm$ and $\tilde{D}^0 \rightarrow K_S\pi^+\pi^-$, can mimic $b \rightarrow u$ mediated signal events (see Fig. 1). The fraction of these events (relative to the number of true D^0 events), defined as $R_{b\rightarrow u} = \frac{N(D^0h^+\pi^-)+N(\overline{D}^0h^-\pi^+)}{N(D^0h^+\pi^-)+N(D^0h^-\pi^+)+N(\overline{D}^0h^+\pi^-)+N(\overline{D}^0h^-\pi^+)}$, has been found to be 0.88 ± 0.02 and 0.45 ± 0.12 in $B\bar{B}$ and continuum MC events respectively.

Studies have been performed on B decays, which have the same final state reconstructed particles as the signal decay (so called peaking background). We identify three possible background sources of this kind: $B^0 \rightarrow \tilde{D}^0K^{*0}$ ($K^{*0} \rightarrow K^+\pi^-$, $\tilde{D}^0 \rightarrow \pi^+\pi^-\pi^+\pi^-$), $B^0 \rightarrow \tilde{D}^0\rho^0$ ($\rho^0 \rightarrow \pi^+\pi^-$, $\overline{D}^0 \rightarrow K_S\pi^+\pi^-$, where ρ^0 is reconstructed as a K^{*0} with a misidentified pion) and charmless events of the kind $B^0 \rightarrow K^{*0}K_SK_S$. The number of charmless background events has been evaluated on data from the $\tilde{D}^0$ mass sidebands, namely $M_{K_S\pi^+\pi^-}$ in the range [1.810, 1.839] or [1.889, 1.920] GeV/c^2; we obtain $N_{peak} = -5 \pm 7$ events, consistent with 0. The selection efficiency for $\tilde{D}^0\rho^0$ and $\tilde{D}^0K^{*0}$ with $\tilde{D}^0 \rightarrow \pi^+\pi^-\pi^+\pi^-$ is $(0.04 \pm 0.02)\%$ or $(0.18 \pm 0.04)\%$, respectively. In the latter case the requirement on α_{K_S} rejects most of the background, while for $\tilde{D}^0\rho^0$ the cuts on ΔE and the particle identification of the $K^\pm$ are the most effective. With these efficiencies, we expect to select about 0.9 $\tilde{D}^0\rho^0$ events and 0.1 $\tilde{D}^0 \rightarrow 4\pi$ events in 371×10^6 $B\bar{B}$ pairs. Hence we assume these background sources can be neglected in our signal extraction procedure; the effects of this assumption are taken into account in the evaluation of the systematic uncertainties. The remaining $B\bar{B}$ background is combinatorial.

We perform an unbinned extended maximum likelihood fit to the variables $m_{\rm ES}$, $\mathcal{F}$ and Δt, in order to extract the signal, continuum and $B\bar{B}$ background yields, probability density function (PDF) shape parameters, and CP parameters. We write the likelihood as

$$\mathcal{L} = \frac{e^{-\eta}\eta^N}{N!}\prod_{\alpha}\prod_{i=1}^{N_\alpha}\mathcal{P}^\alpha(i) , \qquad (3)$$

where $\mathcal{P}^\alpha(i)$ and N_α are the PDF for event i and the total number of events for component α (signal, $B\bar{B}$ background, continuum background). Here N is the total number of selected events and η is the expected value for the total number of events, according to Poisson statistics. The PDF is the product of a "yield" PDF $\mathcal{P}^\alpha(m_{\rm ES})\mathcal{P}^\alpha(\mathcal{F})\mathcal{P}^\alpha(\Delta t)$ (written as a product of 1D PDFs since $m_{\rm ES}$, $\mathcal{F}$ and Δt are not correlated) and of the D^0 Dalitz plot dependent part: $\mathcal{P}^\alpha(m_+^2, m_-^2)$ (where $m_+^2 = m_{K_S\pi^+}^2$ and $m_-^2 = m_{K_S\pi^-}^2$). A detailed description of the resonance structure of the $D^0 \rightarrow K_S\pi^+\pi^-$ Dalitz model, $\mathcal{P}^{\mathsf{Sig}}(m_+^2, m_-^2)$, is given in [11, 12]. In addition, the S-wave component of the $\pi^+\pi^-$ system which is characterized by the overlap of broad resonances uses the K-matrix formalism [13].

The $m_{\rm ES}$ distribution is parametrized by a Gaussian function for the signal and by an Argus function [14] that is different for continuum and $B\bar{B}$ backgrounds. The $\mathcal{F}$ distribution is parametrized using a bifurcated Gaussian distribution for the signal and $B\bar{B}$ background and the sum of two Gaussian distributions for the continuum background. For the signal, $|\Delta t|$ is parametrized with an exponential PDF in which $\tau = \tau_{B^0}$ [9], convolved with a resolution function that is a sum of three Gaussians [15]. A similar parametrization is used for the backgrounds using exponential distributions with effective lifetimes.

The continuum background parameters are obtained from off-resonance data, while the $B\bar{B}$ parameters are taken from MC. The fractions of true D^0 and the ratios $R_{b\to u}$ in the backgrounds are fixed in the fit to the values obtained on data and MC respectively.

Using the definitions 1 and 2 we obtain

$$\begin{aligned}
&\Gamma(B^0 \to D[K_S\pi^-\pi^+]K^+\pi^-) \propto |\mathcal{P}_-^{\mathsf{Sig}}|^2 + \\
&r_S^2|\mathcal{P}_+^{\mathsf{Sig}}|^2 + 2kr_S|\mathcal{P}_-^{\mathsf{Sig}}||\mathcal{P}_+^{\mathsf{Sig}}|\cos(\delta_S + \delta_{D-} - \gamma)\,, \\
&\Gamma(\bar{B^0} \to D[K_S\pi^-\pi^+]K^-\pi^+) \propto |\mathcal{P}_+^{\mathsf{Sig}}|^2 + \\
&r_S^2|\mathcal{P}_-^{\mathsf{Sig}}|^2 + 2kr_S|\mathcal{P}_+^{\mathsf{Sig}}||\mathcal{P}_-^{\mathsf{Sig}}|\cos(\delta_S + \delta_{D+} + \gamma)\,,
\end{aligned}$$

where $\mathcal{P}_+^{\mathsf{Sig}} \equiv \mathcal{P}^{\mathsf{Sig}}(m_+^2, m_-^2)$, $\mathcal{P}_-^{\mathsf{Sig}} \equiv \mathcal{P}^{\mathsf{Sig}}(m_-^2, m_+^2)$ and where $\delta_{D+} \equiv \delta_D(m_+^2, m_-^2)$ is the strong phase difference between $\mathcal{P}_+^{\mathsf{Sig}}$ and $\mathcal{P}_-^{\mathsf{Sig}}$ and $\delta_{D-} \equiv \delta_D(m_-^2, m_+^2)$ is the strong phase difference between $\mathcal{P}_-^{\mathsf{Sig}}$ and $\mathcal{P}_+^{\mathsf{Sig}}$.

Following Ref. [16], we have performed a study to evaluate the possible variations of r_S and k over the $B^0 \to \tilde{D}^0K^+\pi^-$ Dalitz plot. For this purpose we have built a B^0 Dalitz model suggested by recent measurements [7, 17], including $K^*(892)^0$, $K_0^*(1430)^0$, $K_2^*(1430)^0$, $K^*(1680)^0$, $D_{s,2}(2573)^\pm$, $D_2^*(2460)^\pm$, $D_0^*(2308)^\pm$. We have considered the region within 48 MeV/c^2 of the nominal mass of the $K^*(892)^0$ resonance and obtained the distribution of r_S and k by randomly varying all the strong phases ([0,2π]) and the amplitudes (within [0.7,1.3] of their nominal value). The ratio between $b \to u$ and $b \to c$ amplitudes for each resonance has been fixed to 0.4. In the $K^*(892)^0$ mass region, we find that r_S varies between 0.30 and 0.45 depending upon the values of the contributing phases and of the amplitudes. The distribution of k is quite narrow, centered at 0.95 with an r.m.s. of 0.03, and does not show any dependence on the chosen value of the ratio between $b \to u$ and $b \to c$ amplitudes. For these reasons the value of k has been fixed to 0.95 and its variation considered as a systematic uncertainty. On the contrary, r_S will be extracted from data.

We perform the fit for the yields on data extracting the number of events for signal, continuum and $B\bar{B}$, as well as the slope of the Argus function for the $B\bar{B}$ background. The fitting procedure has been validated using simulated events. We find no bias on the number of fitted events for any of the components. The fit projections for $m_{\rm ES}$ is shown in Fig. 2. We find 39±9 signal, 231±28 $B\bar{B}$ and 1772 ± 48 continuum events. In Fig. 2 we also show, for illustration purposes, the fit projections for $m_{\rm ES}$ for a signal-enriched sample.

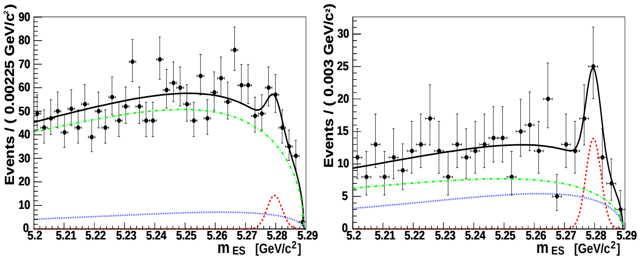

FIG. 2: $m_{\rm ES}$ projection from the fit (left). The data are indicated with dots and error bars and the different fit components are shown: signal (dashed), $B\bar{B}$ (dotted) and continuum (dot-dashed). On the right, with a different binning, $m_{\rm ES}$ projection for a signal-enriched sample.

Based on MC studies, we observe that r_S is overestimated by the fit, causing an underestimate of the error on γ. This feature is similar to the one noted in Ref. [11] and is due to the small signal statistics and the high background level. This problem disappears if r_S is fixed in the fit or if we combine the three-dimensional likelihood function (γ, δ_S,r_S) obtained from this data sample with external information on r_S.

The systematic errors are summarized in Table I. They are related to the $m_{\rm ES}$, $\mathcal{F}$ and Δt PDFs for all the components, to the peaking background assumptions, to the variation of the true D^0 fraction and $R_{b\to u}$ in the background, to the Dalitz distributions of events with no true D^0 and to the assumption made on the factor k. These contributions have been evaluated through a simulation study. The systematic uncertainties from the Dalitz model used to describe true D^0 events has been evaluated from data.

Systematics source	$\Delta\gamma[^\circ]$	$\Delta\delta_S[^\circ]$	$\Delta r_S(10^{-2})$
PDF shapes	1.5	2.5	5.2
Peaking background	0.14	0.12	0.04
True D^0 in the background	0.05	0.03	1.0
$R_{b\to u}$	0.01	1.1	1.9
Dalitz not true D^0	0.31	0.62	0.61
Dalitz background param.	0.03	0.27	0.2
k parameter	0.07	1.2	7.1
Dalitz model for signal	6.5	15.8	6.0
Total	6.7	16.1	11

TABLE I: Systematics uncertainties on γ , δ_S , and r_S.

We extract the experimental three-dimensional likelihood $\mathcal{L}$ for γ, δ_S and r_S from the fit to the data and convolve it with a three-dimensional Gaussian that takes into account the systematic uncertainties. In Fig. 3, we show the 68% probability region obtained for γ assuming different fixed values of r_S and integrating over δ_S. The value of (the fixed) r_S does not affect the central value of γ, but its error. For example, for r_S fixed to 0.35, we obtain $\gamma = (162 \pm 45)^\circ$. On MC, for the same fit configuration, the average error is 39° with a r.m.s. of 12°.

Combining the final three-dimensional PDF with the

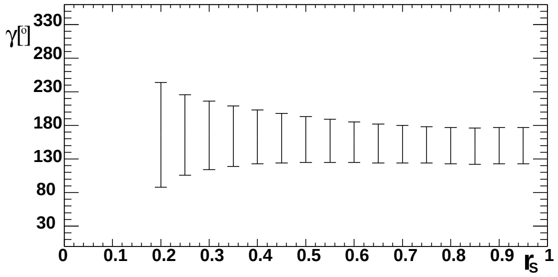

FIG. 3: 68% probability regions obtained for γ, for different values of r_S. A 68% probability region cannot be obtained for values of r_S lower than 0.2. The solution corresponding to a 180° ambiguity is not shown.

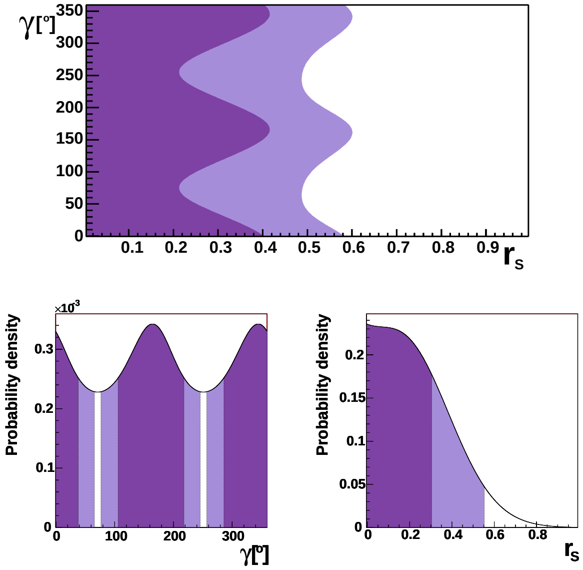

FIG. 4: 68 % (dark shaded zone) and 95 % (light shaded zone) probability regions for the combined PDF projection on the γ vs r_S plane (top), γ (bottom-left) and r_S (bottom-right).

measured PDF for r_S [6], we obtain

$$\begin{aligned} \gamma &= (162 \pm 56)^\circ \text{ or } (342 \pm 56)^\circ; \\ \delta_S &= (62 \pm 57)^\circ \text{ or } (242 \pm 57)^\circ; \\ r_S &< 0.55 \text{ at } 95\% \text{ probability.} \end{aligned} \tag{4}$$

In Fig. 4 we show the distributions we obtain for γ, r_S and γ vs. r_S (the 68% and 95% probability regions are shown in dark and light shading respectively). The one-dimensional distribution for a single variable is obtained from the three-dimensional PDF by projecting out the variable and integrating over the others.

In summary, we have presented a novel technique for extracting the angle γ of the Unitarity Triangle in $B^0 \to \tilde{D}^0 K^{*0}$ ($\overline{B}^0 \to \tilde{D}^0 \overline{K}^{*0}$) with the $K^{*0} \to K^+\pi^-$ ($\overline{K}^{*0} \to K^-\pi^+$), using a Dalitz analysis of $\tilde{D}^0 \to K_S\pi^+\pi^-$. With the present data sample, interesting results on γ and r_S are obtained when combined with the determination of r_S from the study of $\tilde{D}^0$ decays into flavor modes.

We are grateful for the excellent luminosity and machine conditions provided by our PEP-II colleagues, and for the substantial dedicated effort from the computing organizations that support *BABAR*. The collaborating institutions wish to thank SLAC for its support and kind hospitality. This work is supported by DOE and NSF (USA), NSERC (Canada), CEA and CNRS-IN2P3 (France), BMBF and DFG (Germany), INFN (Italy), FOM (The Netherlands), NFR (Norway), MES (Russia), MEC (Spain), and STFC (United Kingdom). Individuals have received support from the Marie Curie EIF (European Union) and the A. P. Sloan Foundation.

---

[*] Deceased

[†] Now at Temple University, Philadelphia, Pennsylvania 19122, USA

[‡] Now at Tel Aviv University, Tel Aviv, 69978, Israel

[§] Also with Università di Perugia, Dipartimento di Fisica, Perugia, Italy

[¶] Also with Universita' di Sassari, Sassari, Italy

[1] M. Gronau and D. London, Phys. Lett. **B253**, 483 (1991); M. Gronau and D. Wyler, Phys. Lett. **B265**, 172 (1991); I. Dunietz, Phys. Lett. **B270**, 75 (1991); I. Dunietz, Z. Phys. **C56**, 129 (1992); D. Atwood, G. Eilam, M. Gronau, and A. Soni, Phys. Lett. **B341**, 372 (1995); D. Atwood, I. Dunietz and A. Soni, Phys. Rev. Lett. **78**, 3257 (1997).

[2] A. Giri, Yu. Grossman, A. Soffer, and J. Zupan, Phys. Rev. **D68**, 054018 (2003).

[3] N. Cabibbo, Phys. Rev. Lett. **10** (1963) 531; M. Kobayashi and T. Maskawa, Prog. Theor. Phys. **49** (1973) 652.

[4] M. Gronau, Phys. Lett. **B557**, 198 (2003).

[5] M. Bona *et al.* (UTfit Collaboration), JHEP **0507**, 028 (2005) [arXiv:hep-ph/0501199]. Updated results available at `http://www.utfit.org/`.

[6] B. Aubert *et al.* (BABAR Collaboration), Phys. Rev. **D74**, 031101 (2006).

[7] G. Cavoto *et al.*, Proceedings of the CKM 2005 Workshop (WG5), UC San Diego, 15-18 March 2005 [arXiv:hep-ph/0603019].

[8] B. Aubert *et al.* (BABAR Collaboration), Nucl. Instr. and Methods **A479**, 1 (2002).

[9] W. M. Yao *et al.* (Particle Data Group), J. Phys. G **33**, 1 (2006).

[10] R. A. Fisher, Annals Eugen. **7**, 179 (1936).

[11] B. Aubert *et al.* (BABAR Collaboration) [arXiv:hep-ex/0607104].

[12] B. Aubert *et al.* (BABAR Collaboration), Phys. Rev. Lett. **95**, 121802 (2005).

[13] V.V. Anisovich and A.V. Sarantsev, Eur. Phys. Jour. **A16**, 229 (2003).

[14] H. Albrecht *et al.* (ARGUS Collaboration), Z. Phys. **C48**, 543 (1990).

[15] B. Aubert *et al.* [BABAR Collaboration], Phys. Rev.

Lett. **99**, 171803 (2007) [arXiv:hep-ex/0703021].

[16] S. Pruvot, M.-H. Schune, V. Sordini, and A. Stocchi [arXiv:hep-ph/0703292], to appear in Proceedings of the CKM2006 workshop, Nagoya, Japan.

[17] F. Polci, M.-H. Schune and A. Stocchi [arXiv:hep-ph/0605129].